CCNY-HEP-96/16
CU-TP-796
MPI-PhT/96-119
hep-lat/9704016
November 1996

Monte Carlo Studies of Two-Dimensional Systems with a θ Term

Jan C. Plefka [a 1]

and

Stuart Samuel [bc 2]

[a] *Department of Physics*
City College of New York
New York, NY 10031, USA

[b] *Department of Physics*
Columbia University
New York, NY 10027, USA

[c] *Max-Planck-Institut für Physik*
Werner-Heisenberg-Institut
Föhringer Ring 6
80805 Munich, Germany

Abstract

A θ term, which couples to topological charge, is added to the two-dimensional lattice CP^3 model and $U(1)$ gauge theory. Monte Carlo simulations are performed and compared to strong-coupling character expansions. In certain instances, a flattening behavior occurs in the free-energy at sufficiently large θ, but the effect is an artifact of the simulation methods.

1) E-mail address: t52@next.nikhef.nl

2) E-mail address: samuel@scisun.sci.ccny.cuny.edu

I. Introduction

Formally, the inclusion of a θ term in a theory does not affect the equations of motion. For this reason, it was once thought that θ terms were irrelevant. In fact, this appears to be the case for the four-dimension $U(1)$ gauge theory. Adding the θ term $\int d^4x F_{\mu\nu}\tilde{F}^{\mu\nu}(x)$ to the action is believed to not affect physics. The situation for a non-abelian theory is different. The importance of the θ term $S_\theta = g^2\theta \int d^4x F^a_{\mu\nu}\tilde{F}^{\mu\nu}_a(x)/(32\pi^2)$ was realized when instantons were uncovered in four-dimensional Yang-Mills theories [1]. Instantons represent barrier-penetration processes between different classical n-vacua. An n vacuum $|n\rangle$ is obtained from the perturbative vacuum through a non-trivial gauge transformation carrying winding number n. Instanton-barrier-penetration effects imply that the true vacua are linear combinations of n vacua. These vacua $|\theta\rangle$ are called θ-vacua [2, 3] and are given by $|\theta >= \sum_{n=-\infty}^{\infty} \exp(in\theta)\,|n\rangle$. In a functional integral, θ-vacua are incorporated by adding the term S_θ to the action. Since S_θ breaks parity, time-reversal invariance and CP symmetry when $\theta \neq 0$ or $\theta \neq \pi$, the strong interactions explicitly violate these symmetries for $0 < \theta < \pi$. In fact, not only do instantons contribute to S_θ but all topological quantum fluctuations also do so. Such topological fluctuations are known to exist because they contribute significantly to the η' mass [4]–[13].

In QCD, phases in the quark mass matrix $\mathcal{M}$ also contribute to CP violation. However, only the combination $\theta_{eff} = \theta + ArgDet\mathcal{M}$ is relevant for strong CP violation for the following reason. Through redefinitions of quark fields, one can eliminate the CP violating phases in the quark mass matrix. However, to eliminate one CP-violating phase, a $U(1)$ axial rotation is used. Via the axial anomaly, $ArgDet\mathcal{M}$ re-emerges as a coefficient of S_θ. Hence, the physical effective theta parameter is θ_{eff}. The strongest constraint on θ_{eff} comes from the electric dipole moment of the neutron. Compatibility with experimental bounds requires $\theta_{eff} \lesssim 10^{-9}$ [14, 15]. The strong CP problem in QCD can then be phrased as the question of how θ_{eff} can naturally be so small. The strong CP problem is thus a fine-tuning issue.

In a pure Yang-Mills theory, the strong CP problem involves vacuum dynamics. Vacuum physics is related to the long-distance behavior of a theory and hence non-

perturbative and strong-coupling effects. For four-dimensional Yang-Mills theories, this regime is not well understood. Thus it is useful to consider simpler systems, such as the two-dimensional CP^{N-1} models. They have features in common with four-dimensional Yang-Mills theories: They are asymptotically free, possess instanton solutions, and have θ vacua.

Insight into the CP^{N-1} models comes from strong coupling expansions [16]-[19], Monte Carlo simulations [20]-[28], and the use of the large N limit [29, 30]. As $N \to \infty$, the CP^{N-1} model becomes a system of N free particles and N free antiparticles, and there is no θ dependence: θ-vacua are degenerate in energy. However, the first $1/N$ correction lifts the degeneracy of the θ-vacua, with the energy separation between θ-vacua being of order $1/N$. The first $1/N$ correction also leads to a quantum-mechanically generated $U(1)$ gauge field. This gauge field produces a linear potential between particles and antiparticles. Hence the system confines, although the string tension, in this approximation, is again of order $1/N$. Actually, it is expected that the confining force becomes stronger and stronger as higher-order $1/N$ corrections are included since the CP^{N-1} models exhibit superconfinement [17]. The dramatic changes in behavior in going from leading order to next-to-leading order are indicative of the singular nature of the $1/N$ expansion in the CP^{N-1} models. The singular nature is also reflected in the fact that strong coupling and $1/N$ expansions do not commute [16, 17, 31]. For this reason, results from Monte Carlo methods should probably be trusted over results from $1/N$ methods.

In the presence of a θ term, G. Schierholz and co-workers in pioneering work have performed Monte Carlo simulations on the CP^3 model.[28] Results for the free energy were interesting and unexpected. For fixed inverse coupling β, a dramatic change in the free energy behavior occurred at a critical value θ_c of θ. The free energy f per unit volume was well represented by

$$f = \begin{cases} a\,(\beta)\,\theta^2 & \theta < \theta_c \\ c\,(\beta) & \theta > \theta_c \end{cases} \quad . \tag{1.1}$$

Hence, for $\theta \geq \theta_c$, the free energy had no dependence on θ. In two dimensions, the string tension $\sigma(e,\theta)$ for external particles of charge e in a theta vacuum $|\theta\rangle$ can be computed from the free energy using $\sigma(e,\theta) = f(\theta+2\pi e) - f(\theta)$.[32] Hence, for $\theta > \theta_c$,

the string tension vanishes for particles of sufficiently small charge. In other words, confinement for small external charges is lost. Furthermore, the simulations in [28] indicated that θ_c went to zero in the continuum limit in which the coupling g goes to zero.

In [19], strong coupling character expansions of the free energy were obtained. Near infinite coupling, no flattening behavior of the free energy like that of Eq. (1.1) was seen. However, at smaller g, a peak in the free energy occurred. Although higher corrections might change this behavior, the strong coupling series provided some support for the form of the free energy given in Eq. (1.1).

Many two-dimensional systems with a $U(1)$ gauge field, such as the Schwinger model, possess a cusp in the free energy at $\theta = \pi$. The cusp signals the spontaneous breaking of CP invariance.[33] At infinite coupling, the lattice CP^{N-1} models also undergo spontaneous CP breaking at $\theta = \pi$.[18] Hence, a phase transition in the CP^{N-1} models at $\theta_c = \pi$ is not unexpected. What is interesting about the numerical studies [28] of the CP^3 model is that, for sufficiently weak coupling, θ_c moves away from π and decreases with decreasing g. This picture suggests that, to obtain a continuum confining theory from the lattice CP^3 model, one must tune θ to zero. This then also suggests that continuum *confining* CP^{N-1} models must have $\theta = 0$.[1] If the analog of this statement were true for a four-dimensional Yang-Mills theory, then the strong CP problem would be solved. In fact, preliminary studies [34] of the free energy of the four-dimensional $SU(2)$ Yang-Mills theory show a free energy behavior similar to the one in equation (1.1). However, in four-dimensional Yang-Mills theories, the string tension is not related to the free energy f. Hence, the analog of the argument for the CP^3 model, namely, that θ must be tuned to zero to obtain confinement, does not necessarily hold. Nonetheless, if θ must be less than θ_c for some other physical reason, and if θ_c goes to zero as $g \to 0$, then the strong CP problem would be solved in the Yang-Mills theories. This is interesting because it has been suggested that the strong CP problem might be solved naturally within the pure Yang-Mills theory.[35] In fact, such a result occurs in a $2+1$ dimensional model: the Yang-Mills sector generates a relaxation field, which acts like the axion

[1] One would still need to explain why confinement is necessary for the continuum limit.

in the Peccei-Quinn mechanism [36, 37, 38]. In ref.[35], criteria were established to determine when such a natural relaxation mechanism arises for theories in arbitrary dimensions. It has not been yet possible to determine whether these criteria are satisfied for four-dimensional Yang-Mills theories.

One unusual feature of the Monte Carlo simulations of ref. [28] is the volume dependence on the free energy for sufficiently large θ. As the volume V increases, θ_c decreases. This leads to a situation in which the free energy differs by large factors as V varies. For example, at $\beta = 2.7$ and θ near π, the free energy on a 46×46 lattice was three times the free energy on a 72×72 lattice. See Figure 3 of ref. [28]. Since quantities, like the free energy, should quickly converge in the thermodynamic limit, there are only three possible explanations:

(i) For sufficiently large θ, there are light, perhaps massless, modes in the system which cause finite-size effects.

(ii) A systematic effect occurs which leads to numerical results that differ from true results.

(iii) There is some unknown explanation not covered by (i) or (ii).

One purpose of the current work is to try to determine whether (i) or (ii) occurs. We perform Monte Carlo simulations on an exactly solvable $U(1)$ lattice gauge theory. By comparing numerical and analytic results, much insight into simulating systems with a θ term is gained. Our results are presented in Section III. We will argue that systematic effects can lead to anomalous flattening behavior in the free energy, as described by Eq. (1.1) for the $U(1)$ lattice gauge theory. In Section II, a general analysis of simulating systems with a θ term is presented. Section II provides a mechanism by which anomalous flattening behavior can arise. In Section IV, a lattice CP^3 model is treated. By comparing Monte Carlo data with analytic strong coupling series from ref. [19], flattening behavior can be shown to be anomalous for at least two simulations. Some additional results and remarks are presented in Section V. In Section VI, a summary and final discussion is given.

II. General Issues Concerning Simulations with θ Terms

In this section, we discuss some issues concerning simulations of an arbitrary lattice theory in the presence of a θ term. In particular, a general error analysis can be carried out. From this analysis, one concludes that, for sufficiently large volumes, a limiting θ exists, beyond which reliable measurements of the free energy cannot be made.

For a fixed V, let $P(Q)$ be the probability of having a configuration with topological charge Q in some system. Let $P_{MC}(Q)$ be the corresponding quantity as measured in a Monte Carlo simulation. Assume that the Monte Carlo updating procedure generates configurations proportional to Boltzmann weights. Below, this assumption is relaxed. If $N_{MC}(Q)$ is the number of times that configurations with topological charge Q arise in such a simulation, then

$$P_{MC}(Q) \equiv \frac{N_{MC}(Q)}{\sum_{Q'} N_{MC}(Q')} \quad . \tag{2.1}$$

In a typical simulation, the measured $P_{MC}(Q)$ differ from the exact $P(Q)$ by small errors $\delta P(Q)$:

$$P_{MC}(Q) = P(Q) + \delta P(Q) \quad . \tag{2.2}$$

With enough measurements, $|\delta P(Q)| \ll 1$. In most systems and the ones considered in this work, $P(Q)$ falls off[2] with Q, so that $P(Q) > P(Q')$ for $|Q| < |Q'|$. A criterion for a simulation to have good statistics is that $\delta P(Q) \ll P(0)$.

Let $f(\theta)$ be the difference between the free energy $\mathcal{F}(\theta)$ of a system with a θ term and the free energy of a system with $\theta = 0$:

$$f(\theta) = \mathcal{F}(\theta) - \mathcal{F}(0) \quad . \tag{2.3}$$

Typically, $f(\theta)$ is an increasing function of θ for $0 \leq \theta \leq \pi$. The free energy difference $f(\theta)$ is constructed from $P(Q)$ using

$$\exp\left(-V f(\theta)\right) = \sum_{Q} P(Q) \exp\left(i\theta Q\right) \quad . \tag{2.4}$$

Normally $P(-Q) = P(Q)$, so that $f(-\theta) = f(\theta)$.

[2]Eventually the falloff is rapid.

In a Monte Carlo simulation, an approximation $f_{MC}(\theta)$ to $f(\theta)$ is obtained by using $P_{MC}(Q)$ in lieu of $P(Q)$:

$$\exp\left(-Vf_{MC}(\theta)\right) = \sum_Q P_{MC}(Q)\exp\left(i\theta Q\right) = \exp\left(-Vf(\theta)\right) + \delta Z(\theta) \quad , \tag{2.5}$$

where

$$\delta Z(\theta) = \sum_Q \delta P(Q)\exp\left(i\theta Q\right) \quad . \tag{2.6}$$

Hence,

$$-Vf_{MC}(\theta)) = \log\left[\exp\left(-Vf(\theta)\right) + \delta Z(\theta)\right] \quad . \tag{2.7}$$

Since $f(\theta)$ is an increasing function of θ, an accurate measurement of $f(\theta)$ for $0 \leq \theta < \theta_0$ is obtained if

$$|\delta Z(\theta)| \ll \exp\left(-Vf(\theta_0)\right) \quad . \tag{2.8}$$

In particular, since $f(0) = 0$ and $|\delta Z(\theta)| \ll 1$, there is always a region near $\theta = 0$ for which $f(\theta)$ can be measured in a Monte Carlo simulation. However, away from $\theta = 0$, Eq. (2.8) implies that accurate results are obtained only if the error $\delta Z(\theta)$ is exponentially small in V. If Eq. (2.8) is satisfied with $\theta_0 = \pi$, then a reliable measurement of $f(\theta)$ can be made throughout the entire fundamental region $0 \leq \theta \leq \pi$.

If the inequality in Eq. (2.8) is not satisfied for some θ_0, then one of several possibilities may arise. If, on one hand, $\exp\left(-Vf(\theta_0)\right)+\delta Z(\theta_0) < 0$ then the argument in the log on the right-hand-side of Eq. (2.7) becomes negative and one will not be able to extract $f(\theta_0)$ from the measurements of the probabilities $P_{MC}(Q)$. In Monte Carlo simulations for such a situation, a growth in the errors of $f_{MC}(\theta)$ will be observed as θ approaches θ_0, and $f_{MC}(\theta)$ will eventually not be measurable. If, on the other hand, $\exp\left(-Vf(\theta_0)\right) + \delta Z(\theta_0) > 0$ then $f_{MC}(\theta)$ will be measurable at $\theta = \theta_0$ but the results will not be accurate.

For sufficiently large V, a value of θ exists beyond which it is impossible to reliable compute $f(\theta)$. If we call this value θ_b, then θ_b is the maximum value of θ_0 for which Eq. (2.8) is satisfied. The value of θ_b depends on the statistical accuracy of the simulation. As V gets larger, θ_b decreases unless an enormously large number of measurements are undertaken to reduce statistical errors. For large V, obtaining enough measurements

becomes, in any practical sense, impossible. Clearly, it is more difficult to measure $f(\theta)$ throughout the entire fundamental region of θ, as V gets larger.

It turns out that in most Monte Carlo simulations, there is a tendency for

$$|\delta P(0)| > |\delta P(1)| > |\delta P(2)| > \ldots \quad . \tag{2.9}$$

The reason for Eq. (2.9) is explained in the next paragraph. For the sake of argument, suppose that $|\delta P(0)|$ is much larger than $|\delta P(Q)|$ for $|Q| \geq 1$. Then, from Eq. (2.8), one concludes that

$$f(\theta_b) \approx \frac{1}{V} |\log |\delta P(0)|| \quad . \tag{2.10}$$

Since Monte Carlo results are reliable for $\theta < \theta_b$,

$$f_{MC}(\theta) \approx f(\theta) \quad \text{for } \theta < \theta_b \quad . \tag{2.11}$$

If, in addition, $\delta P(0) > 0$, then one will find[3]

$$f_{MC}(\theta) \approx -\frac{1}{V} \log \delta P(0) \quad \text{for } \theta > \theta_b \quad , \tag{2.12}$$

so that a constant "flat" behavior in $f_{MC}(\theta)$ will be observed. Although one might expect the statistical error in $f_{MC}(\theta)$ to be the order of $f_{MC}(\theta)$ for $\theta \gtrsim \theta_b$, we have observed in some simulations that the error, as computed by the jackknife method, remains anomalously small. This happens in both the two-dimensional $U(1)$ gauge theory (see Section III) and the CP^3 model (see Section IV). When $\delta P(0) > 0$, $f_{MC}(\theta)$ will smoothly interpolate between the behaviors in Eqs. (2.11) and (2.12) in the region around $\theta \sim \theta_b$. The net result is a form for the free energy which resembles Eq. (1.1). If an error $\delta P(Q)$ for $|Q| > 0$ is almost as large as $\delta P(0)$, then the constant behavior in Eq. (2.12) is replaced by a "slightly wavy" almost flat curve. The above discussion applied to the case $\delta P(0) > 0$. If, on the other hand, $\delta P(0) < 0$, then it will be impossible to measure $f(\theta)$ for $\theta > \theta_b$.

There are various ways to measure $P_{MC}(Q)$. The naive method [39] is to generate configurations proportional to their Boltzmann factor and simply count the number

[3] Note that since $\delta P(0) \ll 1$, the right-hand side of Eq. (2.12) is positive.

$N_{MC}(Q)$ of configurations with topological charge Q, and then use Eq. (2.1). Since the statistical uncertainty $\delta N_{MC}(Q)$ in $N_{MC}(Q)$ is proportional to $\sqrt{N_{MC}(Q)}$,

$$|\delta P_{MC}(Q)| \approx c\sqrt{P_{MC}(Q)} \quad , \tag{2.13}$$

for some constant c.[4] Because $P(Q)$ is a monotonically decreasing function of Q for $Q \geq 0$, the inequalities in Eq. (2.9) tend to be satisfied. In any particular simulation, however, statistical fluctuations may violate Eq. (2.9), particularly if $P(Q)$ is only slightly larger than $P(Q+1)$.[5]

One commonly used Monte Carlo technique [40, 41] is to perform simulations in Q-bins. The topological charges Q are restricted to be in a bin of a certain bin-size. The bins must overlap – usually one takes the bins to overlap for only one Q value. For example, the bins can be taken to be $0 \leq Q \leq \Delta Q$, $\Delta Q \leq Q \leq 2\Delta Q$, $2\Delta Q \leq Q \leq 3\Delta Q$, etc., where ΔQ is a small positive integer. Here, the bin-size is $\Delta Q + 1$. The relative probabilities within a Q-bin are measured by generating configurations which are proportional to their Boltzmann factors but with their topological charges contained in a Q-bin. Overall probabilities are determined from the relative probabilities by matching results at the overlap endpoints of two Q-bins. Compared to the naive method, one generates more configurations with large Q configurations. Hence, errors in $\delta P(Q)$ are relatively reduced for large Q. This tends to enhance the inequalities in Eq. (2.9).

A benefit of the binning technique is that it enables $P(Q)$ to be accurately measured for large Q, even where $P(Q)$ is extremely small. The effect can be spectacular: often $P(Q)$ which are orders and orders of magnitude smaller that $P(0)$ can be measured.

Another simulation method introduces a weight factor $w(Q)$. One then generates Monte Carlo configurations which are proportional to $(the\ Boltzmann\ factor) \times w(Q)$. If $\tilde{N}_{MC}(Q)$ is the number of configurations with topological charge Q which are generated by such a procedure, then Eq. (2.1) is replaced by

$$P_{MC}(Q) \equiv \frac{\tilde{N}_{MC}(Q)\,[w(Q)]^{-1}}{\sum_{Q'} \tilde{N}_{MC}(Q')\,[w(Q')]^{-1}} \quad . \tag{2.14}$$

[4] There might be a weak dependence of c on Q.

[5] This tends to happen when the volume is large and for Q small.

Although any weight $w(Q)$ may be used, the trial-probability-distribution method tries to choose $w(Q)$ so that all Q sectors are "visited" roughly the same number of times.[42] In other words, one guesses a trial probability $P_0(Q)$, which might accurately approximate the true probability distribution $P(Q)$. One then uses $w(Q) = 1/P_0(Q)$. If one were to pick P_0 so that $P_0(Q) = P(Q)$, then a constant distribution in Q for $\tilde{N}_{MC}(Q)$ would be generated (up to statistical fluctuations) and Eq. (2.14) would lead to $P_{MC}(Q) = P_0(Q) = P(Q)$. Like the binning method, the trial-probability-distribution method generates more configurations in the large Q sectors, thereby enabling one to better measure $P(Q)$ for Q large. This method also enhances the inequalities in Eq. (2.9).

Finally, one can combine the above two methods by using a trial probability distribution $P_0(Q)$ with a Q-binning. This trial-probability-binning method is excellent for measuring $P(Q)$ for large Q. However, of the four methods mentioned here, it enhances the inequalities in Eq. (2.9) the most.

In summary, current methods of simulating systems with θ terms tend to generate errors for $P(Q)$ which are ordered as in Eq. (2.9).

None of the methods solve the θ_b barrier problem discussed above between Eqs. (2.8) and (2.13): Assuming that $\delta P(0)$ dominates in the error $\delta Z(\theta)$, one sees that increasing the statistics hardly changes θ_b because of the logarithm and the volume factor in Eq. (2.10). The same statement holds even when $\delta P(0)$ is not the dominant error. One concludes that all simulation methods must fail for sufficiently large θ, if V of the system is large. Cluster algorithms might help a little in this regard. [43]

From the above discussions, the following general guidelines concerning Monte Carlo simulations of systems with a θ term are obtained:

(1) When the volume is sufficiently big, a limiting θ_b arises. For $\theta > \theta_b$, the free energy cannot be reliably measured.

(2) As long as finite-size effects are under control, that is $\xi < V^{(1/d)}$, small-volume results for the measurement of $f(\theta)$ are more reliable than large-volume results. Here, ξ is the correlation length and d is the number of dimensions of the system.

(3) If a flattening behavior of the free energy $f(\theta)$ for large θ is observed, one should be cautious that the result is spurious. In particular, one should try to see whether $|\delta P(0)|$ is bigger than the other $|\delta P(Q)|$.

(4) When $P_{MC}(Q)$ is less than $|\delta P(0)|$, the contribution to $P_{MC}(Q)$ in Eq. (2.5) need not be included. The reason for this statement is that the contribution of $P_{MC}(Q)$ is lost in the "noise" of the error term δZ in Eq. (2.5).

(5) Although the θ_b barrier cannot be overcome, Monte Carlo procedures should emphasize accurate measurements of $P(Q)$ for Q near 0. In particular, the optimal procedure is one for which all $|\delta P(Q)|$ are approximately equal. This minimizes the chances for anomalous flat behavior in $f(\theta)$.

Combining (2) and (3), one obtains another guideline:

(6) If a large-volume simulation shows a flattening effect for $f(\theta)$ for θ sufficiently large, but a smaller-volume simulation does not, one should probably trust the smaller-volume result.

Surprisingly, many previous Monte Carlo studies of systems with θ terms measure $P(Q)$ over many orders of magnitude. Point (4) above says that, although this is not harmful, it is an inefficient use of computer time if one is interested in measuring the free energy. Likewise, point (5) implies that the standard binning and trial-probability methods are not optimal because they enhance the inequalities in Eq. (2.9). The binning method can be improved by doing more measurements in the Q-bin containing $Q = 0$ and less measurements in large-Q Q-bins. Another improvement is as follows. One can adjust $w(Q)$ in Eq. (2.14) so that the errors $|\delta P(Q)|$ are equal (up to statistical effects). It is not hard to show that the optimal $w(Q)$ is $P(Q)$. This corresponds to using a trial-probability function which is the inverse of the true probability. In other words, the optimal weighting method is the antithesis of the trial-probability method and the antithesis of what is commonly employed in Monte Carlo experiments.

III. The Lattice $U(1)$ Gauge Theory

The two-dimensional lattice $U(1)$ gauge theory serves an important test case because computer simulations can be compared to the exact analytic results below. For related Monte Carlo investigations, see refs. [41, 44].

In the lattice formulation of a gauge theory, one assigns an element of the group to each link of the lattice. For the $U(1)$ case, such an element is a phase. The lattice $U(1)$ gauge theory action is

$$S^{U(1)} = \beta \sum_p \left(U_p + U_p^* \right) \quad , \tag{3.1}$$

where U_p is the product of the $U(1)$ link phases around the plaquette p and where β is the inverse coupling.

Define a local topological density ν_p via $\nu_p \equiv \log\left(U_p\right)/(2\pi)$, where $-\pi < \log\left(U_p\right) \leq \pi$. The total topological charge Q is given by $Q = \sum_p \nu_p$. The theta term $S_{\theta \text{ term}}$ is $i\theta Q$, that is, [45]

$$S_{\theta \text{ term}} = \frac{i\theta}{2\pi} \sum_p \log\left(U_p\right) \quad . \tag{3.2}$$

Eq. (3.2) is the lattice analog of the continuum θ-term action $i\frac{\theta}{2\pi}\int d^2x F$.

In $d = 2$ dimensions, gauge theories are exactly solvable even in the presence of a θ term. For periodic boundary conditions, in which case Q is quantized to an integer, the result is [41]

$$Z\left(\theta, \beta, V\right) = \sum_{m=-\infty}^{\infty} \left[z\left(\theta + 2\pi m, \beta\right) \right]^V \quad , \tag{3.3}$$

where

$$z\left(\theta, \beta\right) = \frac{\int_{-\pi}^{\pi} \frac{df_p}{2\pi} \exp(\frac{if_p\theta}{2\pi}) \exp(2\beta\cos(f_p))}{\int_{-\pi}^{\pi} \frac{df_p}{2\pi} \exp(2\beta\cos(f_p))} \quad . \tag{3.4}$$

Here, f_p can be thought of as the field strength for a single plaquette: $U_p = \exp(if_p)$. In the infinite volume limit, the free-energy difference per unit volume $f(\theta)$ is given by

$$f(\theta, \beta) = -\log\left(z\left(\theta, \beta\right)\right) \quad . \tag{3.5}$$

In particular, at $\beta = 0$, one obtains [18]

$$f(\theta, 0) = -\log(\frac{2}{\theta}\sin(\frac{\theta}{2})) \quad , \tag{3.6}$$

when $-\pi < \theta \leq \pi$.

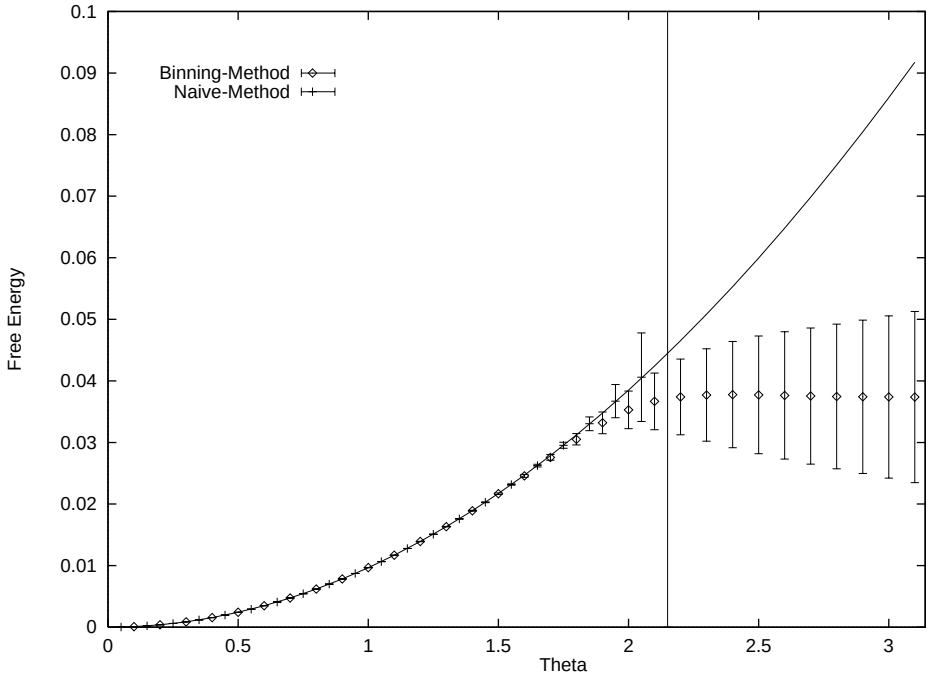

Figure 1: $U(1)$ Free Energy Versus θ at $\beta = 1.0$ for the Naive and Binning Methods.

We have performed Monte Carlo studies of the $U(1)$ gauge theory to gain insight into computer simulations for a system with a θ term. The action consisted of the sum of the actions in Eqs. (3.1) and (3.2). Two values of β were considered: $\beta = 0.0$ and $\beta = 1.0$. Three simulation methods were employed: naive, binning and binning with a trial probability function. Heat-bath updating was used with the naive and binning methods. The Metropolis algorithm was used with the trial-probability-binning method. The trial probability distribution $P_0(Q)$ was chosen to be a gaussian: $P_0(Q) \propto \exp(-kQ^2)$, where the constant k was appropriately selected. After thermalizing the system, the number of sweeps ranged from tens of million to several hundred million. One sweep corresponded to updating once all the link-variables of the lattice. The number-crunching was done on IBM and SUN desktop workstations.

Figure 1 plots the free energy versus θ for $\beta = 1.0$, for a periodic 16×16 lattice. For the naive method, the data points correspond to short horizontal line segments. A total of 75 million updating sweeps were performed. The error bars were computed using a jackknife method [46] by dividing the run into 15 data sets, each of which involved 5 million sweeps. The solid line is the exact analytic result. An-

alytic and Monte Carlo results agree for θ less than 2.1. The agreement, which is excellent, cannot be seen on the scale of Figure 1. For example, at $\theta = 0.5$, $f_{MC} = 0.00242004(53)$ versus $f_{\rm exact} = 0.0024196$, at $\theta = 1.0$, $f_{MC} = 0.0096685(46)$ versus $f_{\rm exact} = 0.0096682$, at $\theta = 1.5$, $f_{MC} = 0.021699(61)$ versus $f_{\rm exact} = 0.021714$, and at $\theta = 2.0$, $f_{MC} = 0.0386(37)$ versus $f_{\rm exact} = 0.0385$, where the statistical uncertainty in the last two digits is displayed in parenthesis.[6] For θ beyond 2.1, error bars grew and the partition function became negative. One sees that the "barrier theta" θ_b is about 2.1. The statistical error in $P_{MC}(0)$ was 3×10^{-5}. Using this error in Eq. (2.10) to estimate θ_b, one finds $\theta_b \approx 2.05$. The agreement of the theoretical θ_b with the Monte Carlo value confirms the data-analysis discussion of Section II. One can also check Eq. (2.13) by seeing whether the ratio of the statistical error of $P(Q)$ to $\sqrt{P_{MC}(Q)}$ remains constant. Even though $P_{MC}(Q)$ varied by eight orders of magnitude, it turned out that the ratio stayed constant to within a factor of 3.

Figure 1 also plots the free energy versus θ and for the binning method, again for $\beta = 1.0$ on a 16×16 lattice. The data points correspond to diamonds. Five bins of bin-size 4 were used. For each bin, 16 million sweeps were performed. Since 5 bins were used, the statistics for this case are comparable to the statistics of the naive method of the previous paragraph. The 16 million sweeps were divided into 20 sets for the jackknife analysis of errors. For $\theta \geq 2.0$, the Monte Carlo data for the free energy dropped below the exact result and became constant. For $\theta \leq 1.7$, the agreement between Monte Carlo data and the analytic result was comparable to the naive-method case, discussed in the previous paragraph. As one can see in Figure 1, the flat behavior in the free energy is anomalous for $\theta > 2.1$ even though the error bars are sizeable. At $\theta = \pi$, the discrepancy with the exact analytic result for f is at the 4σ level.

We also performed a simulation with a trial-probability-binning method, again with $\beta = 1.0$ on a 16×16 lattice. The results were similar quantitatively to the naive case above, except that the Monte Carlo data dropped below the exact result at about 2.1 and then the error bars became enormous for $\theta \geq 2.2$.

In all three of the above runs, the statistical errors in $P(Q)$ were ordered as in

[6] For example, the $\theta = 2.0$ results is $f_{MC} = 0.0386 \pm 0.0037$.

Q	$P_{MC}(Q)$	$P_{\text{exact}}(Q)$	Q	$P_{MC}(Q)$	$P_{\text{exact}}(Q)$
0	1.968226(42) E-01	1.968199 E-01	7	4.51534(28) E-04	4.51495 E-04
1	1.743842(23) E-01	1.743866 E-01	8	6.58573(46) E-05	6.58533 E-05
2	1.212054(16) E-01	1.212086 E-01	9	7.13760(58) E-06	7.13774 E-06
3	6.59478(17) E-02	6.59454 E-02	10	5.64442(51) E-07	5.64463 E-07
4	2.79818(09) E-02	2.79806 E-02	11	3.18299(30) E-08	3.18344 E-08
5	9.20984(42) E-03	9.20931 E-03	12	1.24331(15) E-09	1.24034 E-09
6	2.33452(13) E-03	2.33437 E-03			

Table 1: $P(Q)$ for $U(1)$ Model at $\beta = 1.0$ on a 7×7 Lattice.

Eq. (2.9).

For the binning-method case, one can address the question of whether the flattening behavior is attributable to a value of $P_{MC}(0)$ which is larger than $P(0)$. For a 16×16 lattice, the exact $P(0)$ is 0.179259. The value of $P_{MC}(0)$ for the binning run was 0.179295(72). Thus, $P_{MC}(0)$ was indeed greater than $P(0)$. For the naive run, $P_{MC}(0) = 0.179242(30)$, while for the trial-probability-binning run, $P_{MC}(0) = 0.179192(55)$, and since these two values are below the exact $P(0)$, the anomalous flattening behavior is not expected to arise, in agreement with the Monte Carlo results.

According to Eq. (2.10), one can increase θ_b by decreasing the size of the system. We therefore estimated that if the lattice size was 8, then a reliable measurement of the free energy could be made throughout the entire fundamental θ region. Using a trial-probability-binning method on an 8×8 lattice, reasonable agreement between Monte Carlo data and analytic results was obtained in a 30-million sweep run. For example, at $\theta = 1.0$, $f_{MC} = 0.00980(5)$ versus $f_{\text{exact}} = 0.00967$, at $\theta = 2.0$, $f_{MC} = 0.0382(1)$ versus $f_{\text{exact}} = 0.0385$ and at $\theta = 3.0$, $f_{MC} = 0.089(3)$ versus $f_{\text{exact}} = 0.0814$.

Consider now the infinite-strong-coupling case $\beta = 0.0$. Results for this case were qualitatively similar to the $\beta = 1.0$ case: When the lattice size was sufficiently small, the free energy was measurable over the entire fundamental θ region and the data agreed well with exact analytic calculations. When the lattice size was bigger, the free energy was accurately measurable only for $0 \leq \theta < \theta_b$. For example, a run, which used

θ	F_{MC}	F_{exact}
0.2	1.667250(80) E-03	1.667220 E-03
0.4	6.67569(29) E-03	6.67558 E-03
0.6	1.504550(71) E-02	1.504530 E-02
0.8	2.68107(14) E-02	2.68104 E-02
1.0	4.20200(25) E-02	4.20195 E-02
1.2	6.07374(40) E-02	6.07369 E-02
1.4	8.30438(62) E-02	8.30436 E-02
1.6	1.090390(94) E-01	1.090390 E-01

θ	F_{MC}	F_{exact}
1.8	1.38842(14) E-01	1.38845 E-01
2.0	1.72596(23) E-01	1.72603 E-01
2.2	2.10467(38) E-01	2.10485 E-01
2.4	2.52636(72) E-01	2.52674 E-01
2.6	2.9917(15) E-01	2.9925 E-01
2.8	3.4907(35) E-01	3.4926 E-01
3.0	3.9436(75) E-01	3.9472 E-01

Table 2: Measured and Exact Free Energy for $\beta = 0.0$ on a 4×4 Lattice.

the naive method on a 30×30 lattice and which involved 22 million sweeps, produced good results only for $0 \leq \theta < 0.49$. The barrier value was in agreement with θ_b of 0.5, as computed from Eq. (2.8).[7] When a binning method was used, the free-energy data points began to slip below the analytic results near $\theta \approx 0.45$. A slightly-wavy-but-basically-flat behavior for the free energy was observed for $0.45 < \theta < 0.80$. In this range, the Monte Carlo data was below the exact analytic result at the 2σ level. For $\theta > 0.81$, the error bars become large and the free energy was not measurable. When the lattice size was reduced, the free energy was measurable over a larger θ region. On a 7×7 lattice, we performed a run with the trial-probability-binning method. For the first 180 million sweeps, a graph qualitatively similar to the binning case of Figure 1 was obtained. The free energy was measurable up to $\theta_b \approx 2.1$. For $\theta > 2.1$, the data points fell below the exact result and a flat free-energy curve was produced. From the error in $P(0)$ of $\sim 10^{-5}$, the theoretically predicted value of θ_b from Eq. (2.10) was 2.3. When the run was continued, the flat behavior went away: After a billion sweeps, the data agreed with analytic results for $0 \leq \theta < 2.2$. Beyond 2.2, the data fell slightly below the exact results and the error bars became large at $\theta = 2.7$. For $\theta > 2.7$, the free energy was no longer numerically measurable. Based on Eq. (2.10), the limiting θ_b should be 2.65 for this case, in agreement with the Monte Carlo results. Table 1 displays the kind of accuracy with which $P(Q)$ was measured.

[7] On this large lattice $P(Q)$ decreased slowly for Q near zero, so that the largest statistical error actually occurred for $P(-4)$. This error was 1.4×10^{-5}.

Finally, we reduced the lattice size to 4. In a run using the binning with a probability distribution, the free energy was accurately obtained throughout the fundamental θ region. A run with 525 million sweeps was performed with 2 bins of bin-size 4. Table 2 provides the comparison of Monte Carlo and exact results for the free energy.

The $\beta = 0.0$ results of this section are relevant for the CP^{N-1} models at $\beta = 0$: When $\beta = 0$, the CP^{N-1} models coincide with $U(1)$ gauge theory. A numerical investigation of the CP^3 model at non-zero β is the subject of Section IV.

IV. The Lattice CP^3 Model

Monte Carlo studies of the "adjoint" form of the lattice CP^3 model in the presence of a θ term have been performed in ref. [28]. For our Monte Carlo investigations, we have selected the "auxiliary $U(1)$ field" formulation for two reasons: (1) it allows us to investigate the CP^3 model from a different-but-equally-good form of the lattice action, and more importantly, (2) strong coupling expansions [19] have been obtained for this form of the action, thereby allowing comparisons of Monte Carlo data with analytic results, at least for small inverse coupling β. The CP^{N-1} models without a θ term have been studied by computer simulations in several works. See refs. [20]-[27].

The lattice CP^{N-1} action, which we employ, is

$$S = \beta N \sum_{x,\Delta} \left(z_x^* \cdot z_{x+\Delta} U\left(x, x+\Delta\right) + c.c. \right) \quad , \tag{4.1}$$

where the complex scalar fields z_x^i satisfy $\sum_{i=1}^{N} z_{xi}^* z_x^i = 1$ and where $c.c.$ is the complex conjugate of the first term in Eq. (4.1). Here, the sum over Δ involves the d positively-directed nearest neighbors to x, so that Δ takes on the values e_1, e_2,..., e_d, where e_i is a unit vector in the ith direction. Since we consider the two-dimensional case, $d = 2$. The field $U\left(x, x+\Delta\right)$ is a phase associated with link between x and $x+\Delta$ – it is the same link-variable which appears in the $U(1)$ gauge theory of Section III. To Eq. (4.1), we add S_θ of Eq. (3.2) to obtain the full action. Finally, we treat the $N = 4$ case, i.e., the CP^3 model.

We used the Metropolis algorithm for all degrees of freedom. The z_x^i fields were separated into 4 real and 4 imaginary components. They were updated by performing rotations in each of the 28 planes of the 8-dimensional real vector space. For the $U(1)$

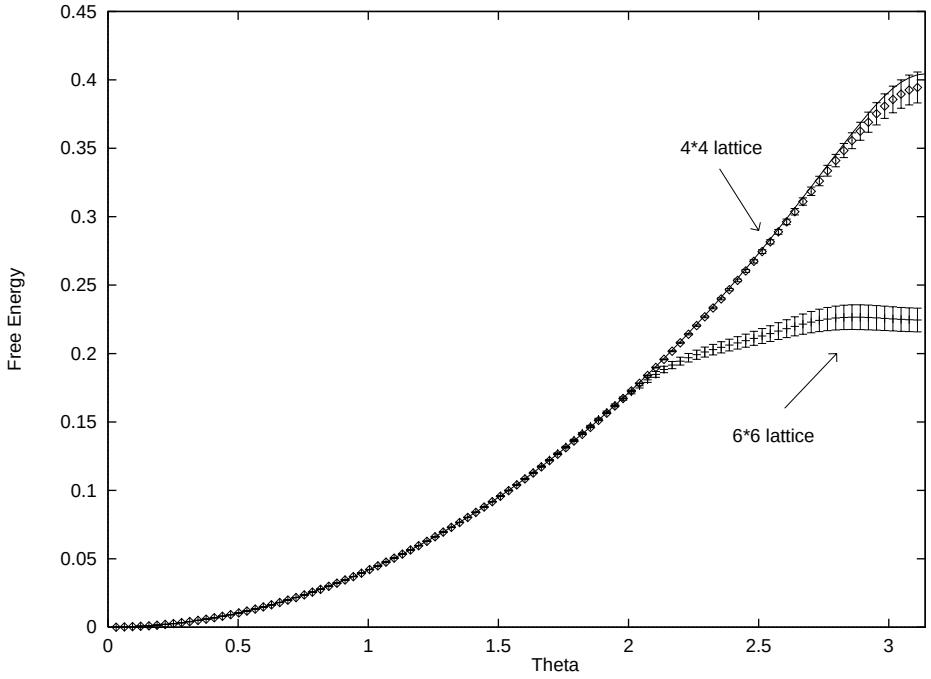

Figure 2: CP^3 Free Energy Versus θ at $\beta = 0.2$ on 4×4 and 6×6 Lattices.

fields, a binning method was used. After each time-consuming update of the z_x^i fields, 10 $U(1)$ updates, as well as Q measurements, were carried out in the fixed z_x^i background. The total number of $U(1)$ sweeps ranged from three to 150 million. Simulations were done for $\beta = 0.2, 0.6, 0.7, 1.0$ and 1.1. The intermediate-coupling cross-over region is around 0.8, so that the latter two β values are in the weak coupling region where continuum scaling should set in.

In some simulations with large volumes, the free energy was not measurable beyond a certain value of θ: error bars became very large or the partition function went negative. The value of θ at which this occurred was in approximate agreement with θ_b obtained using Eq. (2.10). Below, we show results for cases in which the free energy was measurable throughout the entire fundamental θ region or for cases in which a flat behavior was observed.

Figure 2 shows the free energy at $\beta = 0.2$ for 4×4 and 6×6 lattices. The solid line represents the tenth-order strong-coupling character expansion of ref. [19]. At this small value of β, the strong-coupling expansion should be quite close to the exact result. On the 6×6 lattice, an anomalous flattening behavior was observed.

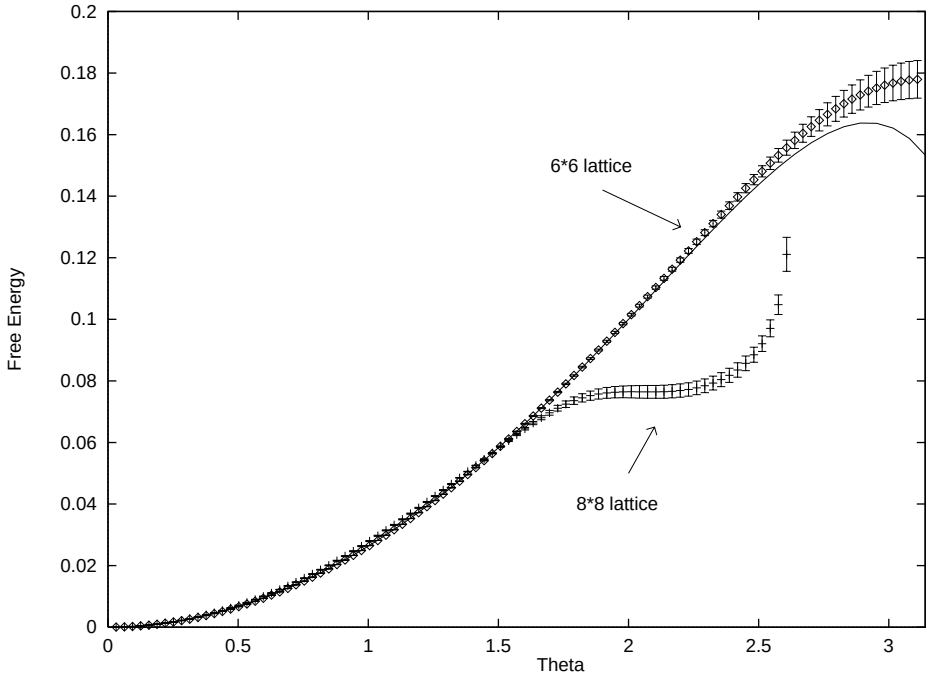

Figure 3: CP^3 Free Energy Versus θ at $\beta = 0.6$ on 6×6 and 8×8 Lattices.

The discrepancy between Monte Carlo data and the strong-coupling series was more than 10σ for θ near π. For some reason, the jackknife error analysis produced error bars which did not come close to overlapping with the true results. Furthermore, Eq. (2.10) predicts that θ_b should be 2.1, so that measurements of the free energy should not be reliable for $\theta > 2.1$. This theoretical estimate for θ_b is close to the point where constant free-energy behavior set in. When the lattice size was reduced to 4, agreement between Monte Carlo data and the strong-coupling series occurred throughout the entire fundamental θ region.

At $\beta = 0.6$, roughly similar behaviors in the Monte Carlo results were obtained except, that on the 8×8 lattice, a flat behavior in the free energy began at $\theta = 1.7$, which turned up at $\theta = 2.5$. The free energy was not measurable beyond $\theta = 2.6$. See Figure 3. Eq. (2.10) predicts that free energy Monte Carlo results should not be trusted for $\theta > 1.75$. For a 6×6 lattice, agreement with the strong-coupling series was obtained up to about $\theta = 2.5$. Beyond that point, the strong-coupling series was slightly below Monte data (at roughly the 1σ level). At $\theta = 2.8$, the strong-coupling expansion of the free energy peaks and for larger θ it decreases, while Monte Carlo

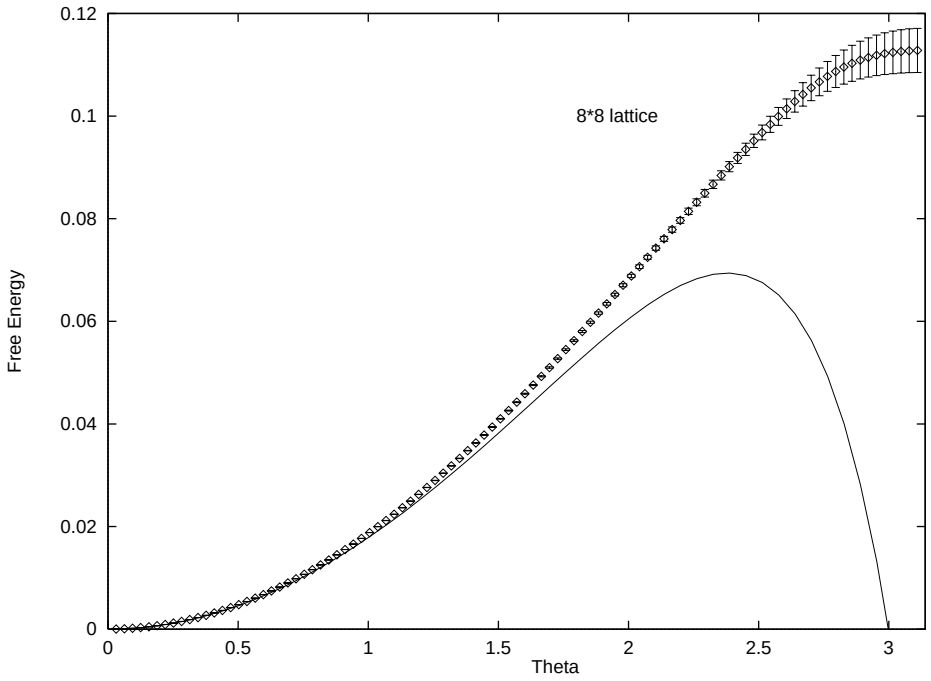

Figure 4: CP^3 Free Energy Versus θ at $\beta = 0.7$ on a 8×8 Lattice.

data continued to increase.

At $\beta = 0.7$, the strong-coupling series peaks at $\theta = 2.4$ and then decreases significantly. Since the free-energy should be a non-decreasing function of θ, higher-order-in-β corrections are probably important in this region, as ref. [19] suggested might be the case. The Monte Carlo data began to rise above the strong-coupling results at around $\theta = 1.2$. See Figure 4. At this value of β, which is in the intermediate coupling region, the Monte Carlo data is to be trusted over the strong-coupling expansion.

At $\beta = 1.0$, which is on the weak coupling side of the intermediate coupling region, a simulation on a 20×20 lattice gave good results throughout the fundamental θ region. Figure 5 displays the free energy versus θ. The solid curve is the fit $f(\theta) = 0.0039 * (1 - \cos(\theta))$. It reproduces the data within error bars. At $\beta = 1.1$, a simulation on a 40×40 lattice also gave good results. The free energy function $f(\theta) = 0.00125 * (1 - \cos(\theta))$ reproduces the $\beta = 1.1$ data well throughout the fundamental θ region. It is interesting that a "cosine" form fits the data for $\beta \geq 1.0$. Such a functional form arises from a topological gas picture [2]. For $\beta < 0.8$, a cosine form did not fit the free energy data.

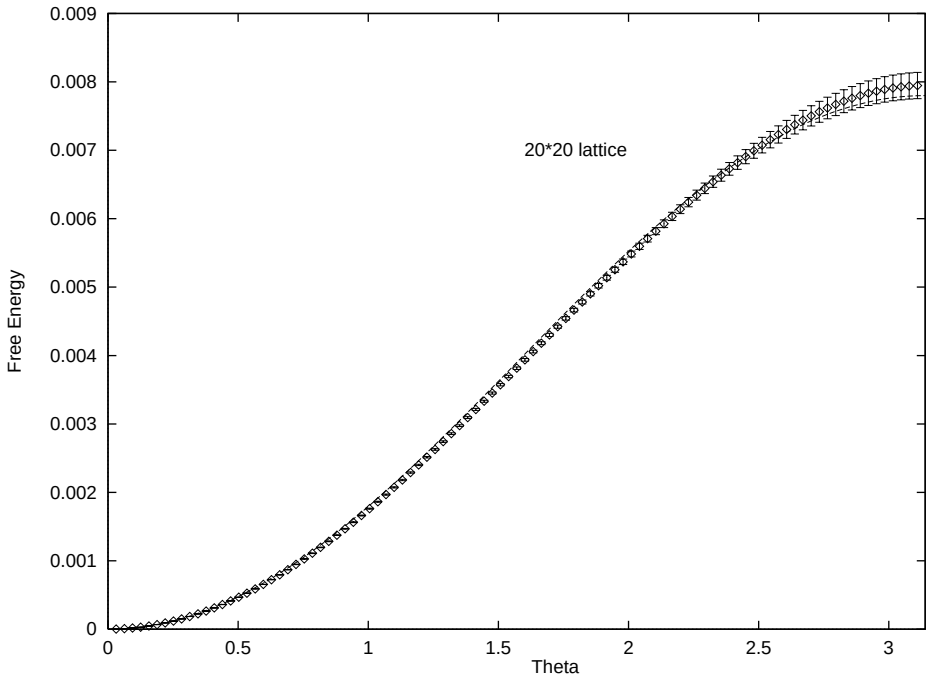

Figure 5: CP^3 Free Energy Versus θ at $\beta = 1.0$ on a 20×20 Lattice and Its Cosine Fit.

V. Remarks

The cosine behavior of the free energy does not agree with the large N limit result, which gives $f_{\text{large } N} = c/N\theta^2$, for some N-independent constant c. The discrepancy might be due to the smallness of N, which is 4 in our case. In other words, higher-order $1/N$ corrections in the large N expansion are important. We believe that this explanation is likely: In the leading zeroeth-order large N expansion, no θ dependence arises in the free energy. The first $1/N$ correction provides the quadratic θ dependence. Hence, the first-order result differs significantly from the zeroeth-order result for large θ and especially near $\theta = \pi$. It is thus quite possible that higher-order $1/N$ corrections contribute to the large θ region and cause the free energy to "curve over" like a cosine function. This would not be the first time that a large N result is anomalous in the CP^{N-1} models.[31, 16, 17] In the zeroeth-order approximation, the CP^{N-1} models do not confine. However, the first $1/N$ correction does lead to confinement.[29, 30] Nonetheless for finite N, the CP^{N-1} models have a property called superconfinement [17] in which charges are so strongly bound that they can-

not be separated by any non-zero distance.[8] Superconfinement corresponds to an infinite string tension. It has been conjectured that summing the $1/N$ series would strengthen the confinement and lead to superconfinement.[17] Probably, quantities in the CP^{N-1} models, which differ greatly in going from the zeroeth order to the first order, such as the free energy for θ away from $\theta = 0$ and the string tension, are not reliably computable in the large N expansion.

An interesting open question is whether there is a phase transition at $\theta = \pi$. At infinitely strong coupling, this is the case.[18] In the strong coupling region, finite volume effects round off the cusp in the free energy when sufficiently small volumes are used to give reliable results near $\theta = \pi$. Hence definitive conclusions cannot be drawn. In the weak coupling region, the cosine function fits are suggestive that the phase transition is absent.

If $f(\theta) = c'\theta^2$, then, as the volume V goes to infinity,

$$\frac{P(Q)}{P(0)} = \exp\left(-\frac{Q^2}{4c'V}\right) \quad . \tag{5.1}$$

This follows from inverting Eq. (2.4):

$$\frac{P(Q)}{P(0)} = \frac{\int_{-\pi}^{\pi} \frac{d\theta}{2\pi} \exp(i\theta Q) \exp\left(-Vf(\theta)\right)}{\int_{-\pi}^{\pi} \frac{d\theta}{2\pi} \exp\left(-Vf(\theta)\right)} \quad . \tag{5.2}$$

As $V \to \infty$, a saddle point expansion of Eq. (5.2) becomes quite accurate. If the minimum of $f(\theta)$ is at $\theta = 0$, one finds

$$\frac{P(Q)}{P(0)} = \exp\left(-a_2\frac{Q^2}{2!} - a_4\frac{Q^4}{4!} - \ldots\right) \quad , \tag{5.3}$$

where

$$a_2 = \frac{1}{Vf^{(2)}(0)} - \frac{f^{(4)}(0)}{2V^2[f^{(2)}(0)]^3} + \frac{[f^{(4)}(0)]^2}{4V^3[f^{(2)}(0)]^5} - \frac{f^{(6)}(0)}{V^3[f^{(2)}(0)]^4} + O(\frac{1}{V^4}) \quad ,$$

$$a_4 = \frac{f^{(4)}(0)}{2V^2[f^{(2)}(0)]^4} + O(\frac{1}{V^4}) \quad , \tag{5.4}$$

where $f^{(n)}(0)$ is the nth derivative of $f(\theta)$ at the origin. Equation (5.3) reduces to Eq. (5.1) if $f^{(n)}(0) = 0$ for $n > 2$.

[8] An interesting side remark is that ref. [19] has shown that superconfinement is lost in the presence of a θ term.

There has been some previous discussion as to whether the Q dependence in $P(Q)$ is gaussian.[47, 48] On one hand, Eq. (5.3) shows that this is the case as $V \to \infty$. On the other hand, if the Q dependence in $P(Q)$ is exactly gaussian then $f(\theta) = c'\theta^2$ for θ in the fundamental θ region, as $V \to \infty$. Since non-quadratic behavior for $f(\theta)$ is usually observed, the Q^4 and higher powers of Q in Eq. (5.3) are important for determining $f(\theta)$. Since the coefficient a_4 of Q^4 falls off as $1/V^3$, large volume systems make it difficult for Monte Carlo simulations to correctly determine the θ dependence of $f(\theta)$ for large θ. One again arrives at the conclusion of guideline (2) of Section II: Small volume results are to be trusted over large volume results for the computation of the free energy. For $\beta > 0.9$, the "cosine" behavior of $f(\theta)$ observed in the Monte Carlo investigations of the CP^3 model imply a non-gaussian behavior of $P(Q)$. In fact, in our simulations of both the $U(1)$ gauge model and of the CP^3 model, small derivations from gaussian behavior of $P(Q)$ were observed for all β values.

VI. Discussion

By comparing Monte Carlo simulations of the $d = 2$ $U(1)$ gauge theory, we have verified the guidelines given in Section II: For sufficiently large volumes, a barrier θ_b arises, beyond which numerical results for the free energy are unreliable. The limiting θ_b can be computed theoretically using Eq. (2.10) with $|\delta P(0)|$ estimated to be the statistical error in $P_{MC}(0)$. When the size of the system is reduced, reliable results are obtained throughout the entire fundamental region for θ. Hence, when small-volume results differ from large-volume results, one should trust the smaller volume results. In some simulations, a flat free-energy behavior is observed for $\theta > \theta_b$. Comparison to exact analytic results demonstrates that the flat behavior is incorrect – the true free energy continues to rise for $\theta > \theta_b$. The flattening effect can be attributed to the error in $P_{MC}(0)$ dominating over the errors in other $P_{MC}(Q)$. The domination of the error in $P_{MC}(0)$ is enhanced by Monte Carlo techniques such as the binning method and the use of a trial probability distribution.

The above conclusions also hold for the "auxiliary $U(1)$ field" formulation of the CP^3 model: When the volume is large, anomalous flat behavior of the free energy is sometimes seen. At $\beta = 0.2$ for the 6×6 lattice run, the flat-energy behavior is

definitely incorrect since a comparison can be made with a reliable analytic strong-coupling expansion. When a smaller lattice size is used, results for the free energy are more accurate and flat behavior is absent. When the inverse coupling β is greater than 0.6, the strong-coupling calculation of the free energy has a peak, but the Monte Carlo data does not. See Figures 3 and 4. At these intermediate values of the coupling, we believe that the peak is an artifact of truncating the series to order ten – higher-order contributions are probably important.

There is a simple physical picture of why a limiting θ_b arises. Current methods for simulating a system with $\theta \neq 0$ are done using the $\theta = 0$ system. There should be a "barrier" separating the two systems. The barrier grows exponentially with the volume V. When V is small or when θ is small, the barrier does not prevent the $\theta = 0$ system from sensing the physics of the $\theta \neq 0$ system. However, as V gets large, the barrier becomes more impenetrable, and for sufficiently large θ, the Monte Carlo simulations do not explore the phase space of the θ-system sufficiently well to give reliable results.

If one applies the guidelines in Section II to the work of ref. [28], one would conclude the following. The simulations of the adjoint form of the lattice CP^3 model in refs. [28] found the absence of a flattening behavior in the free energy for sufficiently small volumes. This is typified in Figure 3 of the first of refs. [28]. Guidelines (2) and (6) say that smaller-volume results are to be trusted over larger-volume results. Hence, one would conclude that the flattening behavior is anomalous. If this is true, it is a result of the probability method which tends to emphasize the error in $P_{MC}(0)$. If the flattening behavior is anomalous, θ_c of ref. [28] should be identified with the barrier theta θ_b. One test of this idea is as follows. Assuming that the statistical errors are approximately the same for all the runs in ref. [28] and that Eq. (1.1) holds, it follows from Eq. (2.10) that $V\theta_c^2$ should be approximately constant for a fixed value of β. At $\beta = 2.5$, for the 28×28, 32×32, 38×38, and 48×48 lattices, $V^{1/2}\theta_c/\pi$ is respectively ~ 20, ~ 21, ~ 21 and ~ 22. At $\beta = 2.7$, for the 56×56, 64×64, and 72×72 lattices, $V^{1/2}\theta_c/\pi$ is respectively ~ 35, ~ 33 and ~ 32. Hence, $V\theta_c^2$ is approximately constant. If the dominance of the error in $P_{MC}(0)$ is the source of the free-energy flattening behavior of refs. [28, 34], one puzzling question arises:

why did all the runs display flattening behavior – one would have expected that, in some runs, the errors in the free energy to become large at θ_c and/or for the partition function to become negative. It is possible that some other subtle systematic effect is playing a role. The discussion here supports explanation (ii) of the Introduction, but one cannot definitively rule out explanation (i), namely, that a massless or light mode arises for θ sufficiently large.

Acknowledgments

We thank Gerrit Schierholz and Peter Weisz for useful discussions. We acknowledge the Max-Planck Institute in Munich, Germany for its considerable support – much of the computer work for this project was carried out on work stations at the Max-Planck Institute. We also thank the ITP of the University of Hanover for use of its computers. This work was supported in part by the PSC Board of Higher Education at CUNY, by the National Science Foundation under the grant (PHY-9420615), and by two Humboldt Foundation grants, one of which is a Lynen-Fellowship.

References

[1] A. Belavin, A. Polyakov,A. Schwartz and Y. Tyupkin, Phys. Lett. **59B** (1975) 85.

[2] C. Callan, R. Dashen and D. Gross, Phys. Lett. **63B** (1976) 334.

[3] R. Jackiw and C. Rebbi, Phys. Rev. Lett. **37** (1976) 172

[4] H. Fritzsch, M. Gell-Mann and H. Leutwyler, Phys. Lett. **47B** (1973) 365.

[5] S. Weinberg, Phys. Rev. **D11** (1975) 3583.

[6] G. 't Hooft, Phys. Rev. Lett. **37** (1976) 8.

[7] E. Witten, Nucl. Phys. **B156** (1979) 269.

[8] G. Veneziano, Nucl. Phys. **B59** (1979) 213.

[9] P. Woit, Phys. Rev. Lett. **51** (1983) 638.

[10] J. Hoek, M. Teper and J. Waterhouse, Phys. Lett. **180B** (1986) 112.

[11] M. Göckeler, A. S. Kronfeld, M. L. Laursen, G. Schierholz and U.-J. Wiese, Nucl. Phys. **B292** (1987) 349.

[12] M. Teper, Phys. Lett. **202B** (1988) 553.

[13] M. Campostrini, A. Di Gaicomo, H. Panagopoulos and E. Vicari, Nucl. Phys. **B329** (1990) 683.

[14] V. Baluni, Phys. Rev. **D19** (1979) 2227.

[15] R. Crewther, P. Di Vecchia, G. Veneziano and E. Witten, Phys. Lett. **88B** (1979) 123.

[16] E. Rabinovici and S. Samuel, Phys. Lett. **101B** (1981) 323.

[17] S. Samuel, Phys. Rev. **D28** (1983) 2682.

[18] N. Seiberg, Phys. Rev. Lett. **53** (1984) 637.

[19] J. Plefka and S. Samuel, *A Strong-Coupling Analysis of the Lattice CP^{N-1} Models in the Presence of a θ Term*, CCNY-HEP-96/7 (May, 1996), hep-lat 9612004.

[20] M. Hasenbusch and S. Meyer, Nucl. Phys. B (Proc. Suppl.) **26** (1992) 610; Phys. Rev. Lett. **68** (1992) 435.

[21] K. Jansen and U.-J. Wiese, Nucl. Phys. **B370** (1992) 762.

[22] U. Wolff, Phys. Lett. **284B** (1992) 94.

[23] A. C. Irving and C. Michael, Nucl. Phys. **B371** (1992) 521; Phys. Lett. **292B** (1992) 392.

[24] A. C. Irving, Nucl. Phys. B (Proc. Suppl.) **30** (1993) 823.

[25] M. Campostrini, P. Rossi and E. Vicari, Nucl. Phys. B (Proc. Suppl.) **30** (1993) 819; Nucl. Phys. B (Proc. Suppl.) **30** (1993) 830.

[26] P. Rossi and E. Vicari, Phys. Rev. **D48** (1993) 3869.

[27] E. Vicari, Phys. Lett. **309B** (1993) 139.

[28] S. Olejnik and G. Schierholz, Nucl. Phys. B (Proc. Suppl.) **34** (1994) 709; G. Schierholz, Nucl. Phys. B (Proc. Suppl.) **37A** (1994) 203.

[29] A. D'Adda, M. Lüscher and P. Di Vecchia, Nucl. Phys. **B146** (1978) 63.

[30] E. Witten, Nucl. Phys. **B149** (1979) 285.

[31] H. E Haber, I .Hinchliffe and E. Rabinovici, Nucl. Phys. **B172** (1980) 458.

[32] M. Lüscher Phys. Lett. **78B** (1978) 465.

[33] S. Coleman, Ann. Phys. **101** (1976) 239.

[34] G. Schierholz, Nucl. Phys. B (Proc. Suppl.) **42** (1995) 270.

[35] S. Samuel, Mod. Phys. Lett. **A7** (1992) 2007.

[36] R. Peccei and H. Quinn, Phys. Rev. Lett. **38** (1977) 1440.

[37] S. Weinberg, Phys. Rev. Lett. **40** (1978) 223.

[38] F. Wilczek, Phys. Rev. Lett. **40** (1978) 279.

[39] G. Bhanot, E. Rabinovici, N. Seiberg and P. Woit, Nucl. Phys. **B230** (1984) 291.

[40] G. Bhanot, S. Black, P. Carter and R. Salvador, Phys. Lett. **183B** (1987) 331.

[41] U.-J. Wiese, Nucl. Phys. **B318** (1989) 153.

[42] M. Karliner, S. Sharpe and Y. F. Chang, Nucl. Phys. **B302** (1988) 204.

[43] W. Bietenholz, A. Pochinsky and U.-J. Wiese, Phys. Rev. Lett. **75** (1995) 4524.

[44] C. Panagiotakopoulos Nucl. Phys. **B251** (1985) 61.

[45] B. Berg and M. Lüscher, Nucl. Phys. **B190** (1981) 412.

[46] I. Montvay and G. Münster, *Quantum Fields on a Lattice*, Cambridge Monographs on Mathematical Physics.

[47] A. S. Hassan, M. Imachi, N. Tsuzuki and H. Yoneyama,
Prog. Theor .Phys. **94** (1995) 861.

[48] A. S. Hassan, M. Imachi, N. Tsuzuki and H. Yoneyama,
Kyushu University preprint KKYUSHU-HEP-26, hep-lat/9508025.